Rheology of Polymer Blend Liquid–Liquid Phase Separation

Abhijit R. Nesarikar†

Department of Chemical Engineering, Northwestern University, Evanston, Illinois 60208

Received March 14, 1995; Revised Manuscript Received June 13, 1995®

ABSTRACT: Liquid–liquid phase separation (LLPS) in hydrogenated and deuterated polybutadiene (HPB and DPB) blends resulted in increases in storage and loss moduli (G' and G'') in the terminal region. For homogeneous blends of monodisperse HPB and DPB we observed $G' \propto \omega^2$ and $G'' \propto \omega$, where ω is the frequency. These exponents of ω decreased due to phase separation. The effects of LLPS, which were larger on G' than G'', increased with quench depth and melt aging time. We performed cooling and heating temperature sweeps on a near-critical and two noncritical blends to locate their LLPS transition temperatures (T_t). The estimated relation between the Flory interaction parameter (χ) and temperature (T) matched satisfactorily with that obtained using small-angle neutron scattering (SANS). The noncritical blends underwent discontinuous transitions and exhibited hysteresis effects, unlike the near-critical blend. Our HPB/DPB blends are better than earlier polystyrene/poly(vinyl methyl ether) blends in verifying the experimental results with the theoretical models. Also, we compared the rheological effects of LLPS transition in blends with those of microphase separation transition (MST) in block copolymers.

Introduction

We have studied liquid–liquid phase separation (LLPS) in blends of model hydrogenated polybutadiene (HPB) and deuterated polybutadiene (DPB) with dynamic shear behavior. In a master plot or reduced plot for a blend, storage and loss moduli (G' and G'') are larger for phase-separated states than those for homogeneous states. Similar results were seen in the blends of polystyrene (PS) and poly(vinyl methyl ether) (PVME).[1–7] Mazich and Carr[1] and Ajji et al.[2,4] verified the rheologically obtained transition temperature (T_t) for PS/PVME systems with cloud-point data, and for similar systems Mani et al.[5] located the T_t with rheology as well as a fluorescence technique. Theoretical analyses to explain the rheological effects were done by Onuki[8] and Ajji and Choplin.[9]

Unlike the earlier studies, we chose blends of model-HPB/model-DPB, for which LLPS is described by the Flory–Huggins lattice model. The use of well-characterized model blends allowed us to compare our results with the small-angle neutron scattering (SANS) results[10,11] based on the Flory–Huggins model. We systematically varied the volume fraction of HPB (φ) and the temperature of a HPB/DPB blend and mapped those variations on the blend phase diagram. The principle behind the rheology of LLPS is as follows.

Rheological Principle. For a monodisperse polymer, in the terminal region, $G' \propto \omega^2$ and $G'' \propto \omega$, where ω is the frequency of oscillation. The terminal region is the low-ω end of the G' and G'' vs ω plot such that $\omega\tau_t << 1$, with τ_t being the terminal relaxation time of the polymer.[12] The same behavior is also exhibited by a homogeneous blend of two monodisperse polymers,[12] which we refer to as the *homogeneous rheological* behavior. If the blend phase separates, values of G' and G'' increase, and the exponent of G' vs ω is less than 2 and that of G'' vs ω less than 1. We call this the *heterogeneous rheological* behavior or the *deviations* from homogeneous rheological behavior. In our experiments, we employed small-amplitude dynamic shear experiments in the terminal region,[1–7] thus avoiding *shear-induced* mixing.[13] This made the rheological technique comparable to quiescent techniques for LLPS, like small-angle neutron scattering and turbidity observations.

In a typical blend, LLPS is brought about by changing its temperature.[1–7] The change in temperature also causes changes in rheological properties (G' and G'') of the homogeneous state, though the exponents of 2 in G' vs ω and 1 in G'' vs ω are maintained. These changes can be eliminated by time–temperature superposition[12] of different G' vs ω and G'' vs ω curves at different temperatures. The resulting plot is the *reduced* plot[12]—a plot of $b_T G'$ and $b_T G''$ vs $a_T\omega$—for the homogeneous system, where a_T and b_T are the horizontal and vertical shift factors. As the temperature range in our experiment was small, values of b_T are close to 1 and are neglected. In a reduced plot, the highest temperature at which the deviations from homogeneous rheological behavior are seen is the transition temperature (T_t). Unlike the reduced plot, the modified Cole–Cole plot or the G' vs G'' plot[14] does not involve shifting of data. All the G' vs G'' curves for the homogeneous temperature superimpose, while the curves for the heterogeneous temperatures deviate. The highest temperature exhibiting the deviations represents the transition temperature (T_t).

Thermodynamics. In our experiments, a DPB is nothing but an HPB with some of its hydrogen atoms being replaced by deuterium atoms; the fraction of HPB deuterated is denoted by f^d. We do not consider in detail, the changes in thermodynamic properties of an HPB due to partial deuteration;[10,11] that is, we treat a DPB as its equivalent HPB. An HPB is a poly(ethylene-*co*-butene-1), and we consider it to be a copolymer of monomers A and B, where A and B are linear and ethyl branched C_4H_8 repeat units, respectively. The fraction of monomer B, also known as composition, is y; thus, the copolymer can be represented as $A_{1-y}B_y$. A and B repel each other; therefore, an A-rich HPB can phase separate from a B-rich HPB in their mixture, when the temperature of the system is decreased. Thus, the system exhibits upper critical solution temperature (UCST). The Flory interaction parameter between the two monomers, χ_m, is the measure of repulsive interaction between the two monomers. For two copolymers, H and D, compositions are y_H and y_D. In a blend of H

† Current address: Department of Materials Science and Engineering, Northwestern University, Evanston, IL 60208.

® Abstract published in *Advance ACS Abstracts,* September 1, 1995.

0024-9297/95/2228-7202$09.00/0

Table 1. Polymer Characteristics

HPB nomenclature	y	N_w	N_w/N_n
HPB37	0.37	772	<1.1
DPB58 ($f^d \approx 0.4^a$)	0.58	930	<1.1

[a] Fraction of HPB deuterated.

Table 2. Blend Characteristics

blend	blend components[a]	φ
H37/D58-25	HPB37 and DPB58	0.25
H37/D58-50	HPB37 and DPB58	0.50
H37/D58-75	HPB37 and DPB58	0.75

and D, the volume fraction of the H copolymer is φ; therefore, the volume fraction of D is $1 - \varphi$. The Flory interaction between H and D chains is χ, and $\chi = \chi_m(y_H - y_D)^2$.[15] The average composition of a blend is $\bar{y} = \varphi y_H + (1 - \varphi)y_D$. In the Results and Discussion section we develop a phase diagram for our blends with the help of Flory–Huggins lattice theory.

Experimental Section

HPB and DPB were prepared from anionically polymerized polybutadiene precursors.[16-18] Molecular weight characterization of the polybutadienes was done with gel permeation chromatography (GPC), and the composition (y) was determined by IR on polybutadiene precursors. Characteristics of the HPB used in this study are given in Table 1. Weight-average and number-average degrees of polymerization are N_w and N_n, and N_w/N_n is the polydispersity. Weight-average and number-average molecular weights can be obtained by multiplying N_w and N_n by the molecular weight of the repeat unit, which is $-C_4H_8-$.

Rhee[17] blended HPB and DPB by dissolving them in cyclohexane and precipitating with excess (5:1) ice-cold methanol with 1.2 g L^{-1} Santanox (Monsanto Co.) as an antioxidant. The individual components in the blends were not available for examination. Details of the blends are summarized in Table 2; names used for the blends indicate their components and the volume fraction of HPB; for example, H37/D58-25 has HPB37 and DPB58, with the volume fraction of the HPB (φ) being 25%.

All the blends were checked by differential scanning calorimetry (DSC) to be amorphous above 20 °C; that is, their DSC curves did not show crystallization or melting peaks. Thus, we eliminated the possibility of crystallization for the experimental temperature range of 20–80 °C. The glass transition temperatures of all the copolymers are less than −50 °C,[19] therefore, all the blends were in their equilibrium liquid state, and no effects of glass transition were expected on the experiments.

Dynamic shear experiments were done with a 30-mm-diameter cone-and-plate arrangement in a Bohlin VOR melt rheometer; cone angle was 2.5°. A frequency range of 0.0314–125.66 rad s^{-1} was used, and the amplitude of oscillation was maintained at less than 2 mrad. The test samples were molded under vacuum at about 150 °C, so that no air bubbles were present. To determine the transition temperature, each test blend was first heated to a maximum temperature, and then the temperature was decreased in desired step sizes to a minimum temperature during the *cooling cycle* and increased similarly during the *heating cycle*. Thermal equilibrium at each temperature was ensured by maintaining the sample at that temperature for more than 20 min before starting the frequency scans. To ensure thermodynamic equilibrium—or rather near-equilibrium—two frequency scans were performed, first descending and then ascending. Typically, there was a good match between the two data, showing that time effects (or the effects of time after quenching) were minimal. A maximum error of ±1 °C in the temperature control was determined by inserting an external thermocouple between the cone and the plate.

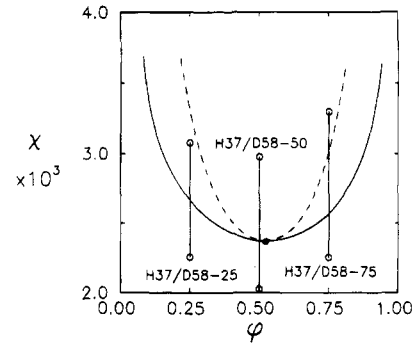

Figure 1. Binary phase diagram for HPB37 and DPB58 using the relation $\chi = 1.82/T - 0.00313$. The vertical lines at volume fractions (φ) of 0.25, 0.5, and 0.75 correspond to the temperature sweeps.

Results and Discussion

In Figure 1, the phase diagram, volume fraction of HPB (φ) is plotted against χ. The temperature–χ relationship is given by $\chi = a/T + b$, where T is in absolute units, $a = 1.82$, and $b = -0.003\,13$. Later in this section, we will discuss the origin of the a and b values. The solid line (binodal) in the phase diagram divides the one-phase (below the solid line) and two-phase (above the solid line) regions. It is derived by equating the chemical potentials of the components (HPB and DPB) in both the phases. This results in two independent equations and two unknowns, which are volume fractions of HPB in both the phases (φ). For a system at a particular value of χ, the two equations are solved numerically to obtain the two φ values. The computation is done for a range of χ values with a certain step size, $\Delta\chi$. The transition χ (χ_t) is defined such that, for $\chi > \chi_t$, the system is phase separated and, for $\chi < \chi_t$, it is homogeneous. The plot of χ_t vs φ is the binodal line. More details of the calculation can be obtained somewhere else.[20,21]

The dotted line (spinodal) separates the spinodal region from the metastable region, which is encloded by spinodal and binodal lines. In the spinodal region, a one-phase mixture of the two components is inherently unstable and undergoes instantaneous phase separation. On the other hand, in the metastable region a one-phase mixture may be stable for a finite time; the nucleation-and-growth energy barrier prevents the phase separation for that time. The equation of the spinodal line is $2\chi_s N\varphi(1 - \varphi) = 1$, where $N = N_H N_D/((1 - \varphi)N_D + \varphi N_H)$ and χ_s is the spinodal χ. At the critical point (the filled dot in Figure 1), defined by χ_c and φ_c, the binodal and spinodal coincide, and the metastable region is absent. The T_c, χ_c, and φ_c values are the values of T, χ, and φ at the critical point. The equations for the critical point are $\chi_c = (N_H^{-1/2} + N_D^{-1/2})^2/2$ and $\varphi_c = N_D^{1/2}/(N_H^{1/2} + N_D^{1/2})$.

In Figure 1, the blend H37/D58–50 has a volume fraction ($\varphi = 0.50$) close to the critical volume fraction ($\varphi_c = 0.523$); therefore, it is called a near-critical blend. Due to the asymmetric nature of the phase diagram, $\varphi_c \neq 0.5$. The other two blends, H37/D58–25 and H37/D58–75, are noncritical. Vertical lines in the phase diagram represent the heating and cooling cycles. Temperature of the H37/D58–25 blend was varied between 20 and 65 °C; the H37/D58–50 blend, between 25 and 80 °C; and the H37/D58–75 blend, between 16 and 65 °C.

The transition between one phase and two phases occurs at the binodal line. The transition temperature

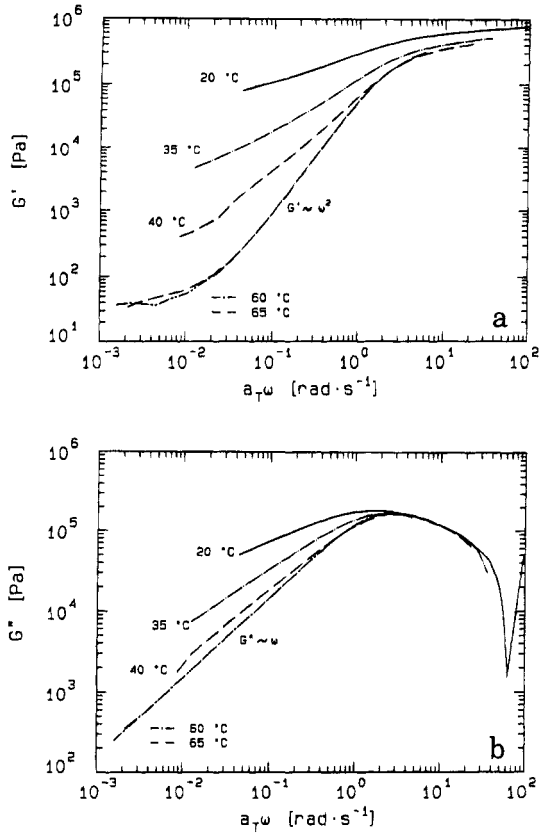

Figure 2. Frequency sweeps at different temperatures for the H37/D58−75 blend. The blend was heated from 20 to 65 °C. The reference temperature (T_0) for the reduced plot is 20 °C. (a) log−log plot of storage modulus (G') vs $a_T\omega$. (b) log−log plot of loss modulus (G'') vs $a_T\omega$.

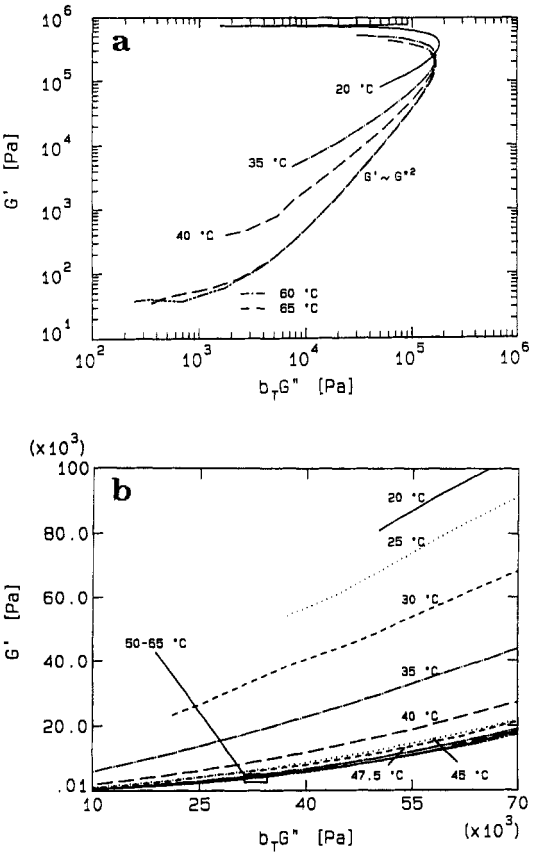

Figure 3. Plot of G' vs G'' for the H37/D58−75 blend. The blend was heated from 20 to 65 °C. (a) log−log plot, also referred to as the modified Cole−Cole plot. (b) Linear plot, to locate the transition temperature. The transition temperature is between 47.5 and 50 °C.

is denoted by T_t, and χ at this transition, by χ_t. When a noncritical blend, say H37/D58−75, is heated from its two-phase region, it homogenizes at T_t. However, if it is cooled from its one-phase region into the metastable region ($T_s < T < T_t$ or $\chi_s > \chi > \chi_t$), the phase separation does not occur instantaneously. Also, phase separation does not take place at T_t but at a temperature less than T_t. This requirement of finite undercooling for phase separation is a characteristic of noncritical blends.[22] Unlike a noncritical blend, a critical blend does not exhibit a metastable region. As a result, when a critical system is cooled, at T_c it enters into the spinodal region and undergoes instantaneous phase separation; no undercooling is required. The H37/D58−50 blend, a near-critical blend, exhibits more critical properties than the noncritical properties.

To study the phase separation rheologically, we show reduced plots of G' and G'' vs ω for one of the noncritical blends, H37/D58−75, that was heated from its heterogeneous to homogeneous phase (Figure 2). The reduced plots (i.e., G' and G'' vs $a_T\omega$) are obtained by time−temperature superposition[12] of G' and G'' vs ω plots at different temperatures. The reference temperature for the reduced curve is 20 °C. The homogeneous rheological behavior is seen for 60 and 65 °C, because the exponent of G' vs ω is 2 and G'' vs ω is 1. For the remaining three temperatures—40, 35, and 20 °C—the exponent of G' vs ω is less than 2 and that of G'' vs ω is less than 1. For the phase-separated blend, as the temperature was increased for the quench depth was decreased, the system approached the homogeneous rheological behavior.

Time−temperature shifting is considered successful if the curves, G' and G'' vs ω, at different temperatures coincide. Polymers and their mixtures, in their homogeneous state, show successful time−temperature superposition.[12] However, for phase-separated polymer mixtures time−temperature superposition fails.[14] Thus, the failure of time−temperature superposition for the 20−40 °C range indicates that the system is liquid−liquid or liquid−solid phase separated. However, when the blends were tested with DSC, no liquid−solid phase separation or crystallization was observed in the temperature ranges of interest. Thus, liquid−liquid phase separation was the reason for the heterogeneous rheological behavior. Also, effects of LLPS were more prominent on G' than G'' (Figure 2); that is, the relative increase in G' was more than that in G''.

As the time−temperature superposition failed for the heterogeneous phase, the curves did not coincide with each other. While preparing the reduced curves, we shifted the phase-separated curves to coincide the maxima in G'' vs ω curves to that of the homogeneous phase reduced curve. Therefore, a failure of superposition was seen toward the low-ω end of the curve. This failure of time−temperature superposition, which indicates LLPS, makes the use of time−temperature superposition nonrigorous.

An alternative method suggested by Chuang and Han[14] is to plot G' vs G'', where effects of temperature and frequency are eliminated; the plot is known as a modified Cole−Cole plot. This plot for H37/D58−75 (heating) is shown in Figure 3a. The homogeneous phase curves for 60 and 65 °C coincide, but the heterogeneous phase curves for 20, 35, and 40 °C deviate from them. The highest temperature exhibiting the deviation represents the transition temperature T_t. A better

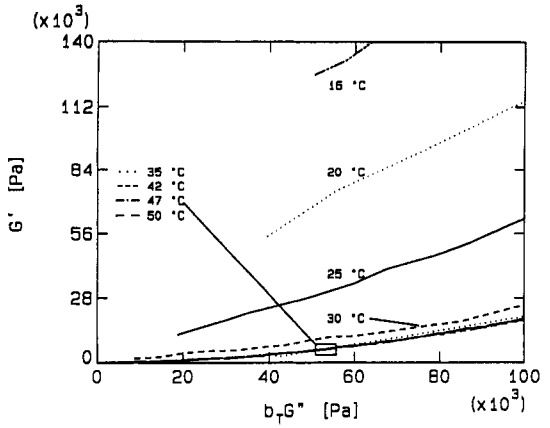

Figure 4. Linear G' vs G'' plot for cooling of H37/D58-75 to locate the transition temperature, which is about 32 °C.

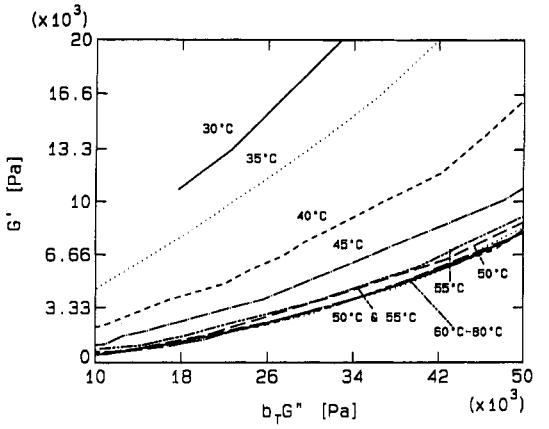

Figure 5. Linear G' vs G'' plot for heating of H37/D58-50 to locate the transition temperature, which is between 55 and 60 °C. The location of the transition point is made difficult by the continuous nature of the transition for this near-critical blend.

determination of T_t is done with a linear G' vs G'' plot as shown in Figure 3b, where the rheological LLPS effects are magnified, and the determination of T_t is easier. The homogeneous rheological behavior is seen from 50 °C and above, and the deviations from the behavior are seen from and below 47.5 °C. Thus, the transition point for H37/D58−75 is 49 ± 1.5 °C. We used similar expanded linear G' vs G'' plots to locate the transition points of the remaining two blends. The detailed analysis can be obtained elsewhere.[21]

When the H37/D58−75 blend was cooled from the one- to the two-phase region, the phase transition did not occur at T_t but at a temperature lower than T_t (Figure 4). Homogeneous rheological behavior is seen for 35, 42, 47, and 50 °C, and deviations from it are seen for 30, 25, 20, and 16 °C. This requirement of undercooling for a one- to two-phase transition is a characteristic of a noncritical transition.[22] From the phase diagram (Figure 1), the spinodal temperature of the blend is 23 °C. Therefore, the phase transition, which occurred between 30 and 35 °C, was by heterogeneous nucleation and growth. It is widely accepted that for moderate undercoolings phase separation takes place by heterogeneous and not homogeneous nucleation.

In a symmetric phase diagram, for two blends with volume fractions (φ) symmetric about the critical volume fraction (φ_c), transition temperatures (T_t) of the two blends are the same. The phase diagram for our blends (Figure 1) is not perfectly symmetric but is near-symmetric. Therefore, T_t's of the two blends are slightly different. The value of χ_t for H37/D58−25 is 2.568 × 10^{-3}, and that for H37/D58−75, 2.520 × 10^{-3}. Therefore, one expects T_t for the former to be smaller than that for the latter, which is 49 ± 1.5 °C. We obtained T_t for H37/D58−25 to be 46 ± 1.5 °C.[21] Similar to the H37/D58−75 blend, the H37/D58−25 blend exhibited the properties of noncritical blends.

Figures 5 and 6 are the heating and cooling data for the near-critical blend, H37/D58−50. For the heating case (Figure 5) the transition point is 57.5 ± 2.5 °C, and for the cooling case it is 52.5 ± 2.5 °C. The difference between the two transition points or undercooling is smaller than that for the noncritical blend, H37/D58−75. For a noncritical blend the undercooling diminishes as its volume fraction (φ) approaches φ_c, and for a critical blend the undercooling is zero.[22] Also, a critical blend exhibits a *continuous transition*;[21] that is, the changes in the physical properties of the blend are continuous at the transition. Unlike a critical blend, a noncritical blend undergoes a *discontinuous transition*.[21]

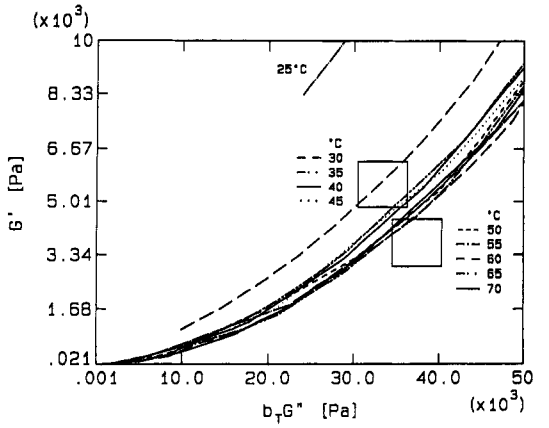

Figure 6. Linear G' vs G'' plot for cooling of H37/D58−50 to locate the transition temperature, which is about 52.5 ± 2.5 °C.

As the blend becomes more and more noncritical or the difference between the blend φ and φ_c increases, the transition becomes increasingly discontinuous. In Figures 5 and 6, due to the continuous nature of the transition, determination of T_t is difficult; the difficulty increases as one approaches the critical point.

To illustrate the properties of critical and noncritical blends more clearly, we plotted G' vs T at a constant $a_T\omega$ (Figure 7a,b). The basis for the development of the plot is the time−temperature superposition as shown in Figure 2. Though the time−temperature superposition is nonrigorous for phase-separated systems, use of the G' vs T plot (Figure 7) to explain the critical and noncritical blend properties is more clear and concise. Figure 7a is for one of the noncritical blends—H37/D58−75. For the heating of the noncritical blend the horizontal line of $G' = 5 \times 10^5$ Pa from 49 to 70 °C represents the homogeneous phase. The transition temperature (T_t) is 49 ± 1.5 °C, below which the increase in G' is attributed to the phase separation. For the cooling case the system is homogeneous below T_t = 49 °C, and phase separation takes place at 32 ± 2.5 °C, which represents an undercooling of 17 °C. The presence of undercooling is also known as the *hysteresis* effect,[22] which is a definitive indication of liquid−liquid phase transition and makes the determination of transition temperature reliable.[13] Unlike the noncritical transition (Figure 7a), the near-critical transition of H37/D58−50 (Figure 7b) does not show a significant

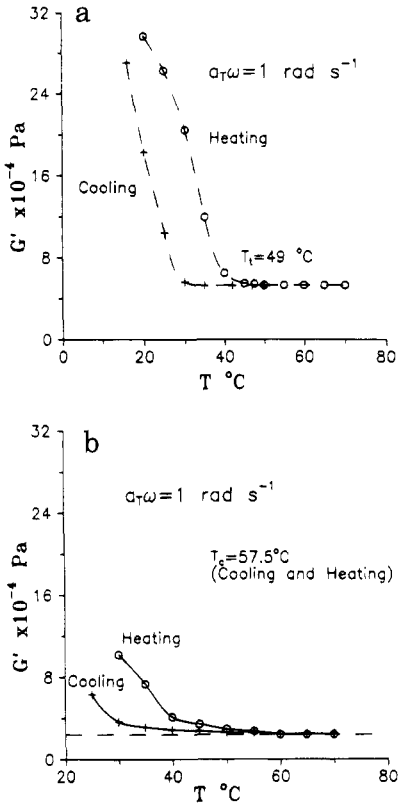

Figure 7. Linear plots of G' vs T at $a_T\omega = 1$ for heating and cooling cycles. (a) The noncritical blend H37/D58−75. (b) The critical blend H37/D58−50.

undercooling or hysteresis. Also, the comparison of the two plots shows that the noncritical transition is abrupt or discontinuous, and the near-critical transition is gradual or less discontinuous. Due to the gradual change in G' at the transition, determination of T_t for the near-critical blend is difficult (Figure 7b). For the noncritical blends, discontinuities were also observed in $\log(a_T)$ vs T^{-1} plots; however, discontinuity was not present for the near-critical blend.[21] Similar results were observed in the PS/PVME blend studies; Mazich and Carr[1] and Ajji et al.[4] reported discontinuities in noncritical systems, and Stadler et al.[3] observed no discontinuity for their critical blend.

The transition point for the near-critical blend H37/D58−50 is 57.7 ± 2.5 °C; for the noncritical blend H37/D58−75, 49 ± 1.5 °C; and for the noncritical blend H37/D58−25, 46 ± 1.5 °C. Using the Flory−Huggins analysis, which is described at the beginning of this section, we obtained the χ_t for H37/D58−50 to be 2.368 × 10^{-3}; for H38/D58−75, 2.520 × 10^{-3}; and for H38/D58−25, 2.568 × 10^{-3}. The least-squares fit for χ vs T^{-1}, with T in absolute units, led to $a = 1.82$ and $b = -3.13 \times 10^{-3}$ in $\chi = a/T + b$.

Study of SANS[10,11] revealed that the liquid−liquid phase separation properties of a HPB/HPB blend change, if one of the components is deuterated. For an HPB1/HPB2 blend, $\chi = \chi_m(y_1 - y_2)^2$, where y_1 and y_2 are the compositions of the two copolymers and χ_m is the Flory interaction parameter between the linear- and branched-C_4H_8 units. If one of the HPBs is deuterated, besides $y_1 - y_2$, χ also depends on isotopic interactions, microstructure interactions, and interactions between the hydrogenated and deuterated monomers.[10] If the less-branched HPB is deuterated, χ decreases, and if the highly branched HPB is deuterated, it increases. In our analysis we neglected the effects of deuteration. However, for consistency, we chose compositions similar to those of the HPB/DPB blends of Graessley et al.[11] For their HPB38/DPB52 blend, with $\bar{y} = 0.45$, $\chi = 7.6 \times 10^{-4}$ at 167 °C and $\chi = 10.1 \times 10^{-4}$ at 109 °C; therefore, $\chi = 0.72/T - 8.87 \times 10^{-4}$. As $y_D - y_H = 0.14$, $a_m = 36.95$ and $b_m = -0.045$ in $\chi_m = a_m/T + b_m$. In our analysis $a = 1.82$ and $b = -3.13 \times 10^{-3}$; for $y_D - y_H = 0.21$ we obtained $a_m = 41.25$ and $b_m = -0.071$. The comparison of a_m and b_m between the two studies is satisfactory.

It is important to note here that, as Graessley et al.[23] have shown, χ_m is a function of T and $\bar{y}'$, where $\bar{y}' = {}^1/_2(y_H + y_D)$. They observed increases in χ_m with increasing $\bar{y}'$. However, in our analysis $\bar{y}' = 47.5$, which is close to $\bar{y}' = 0.45$ for HPB38/DPB52 of Graessley et al.,[11] and the effects of $\bar{y}'$ on χ_m can be neglected. Also, Rhee and Crist[10,24] observed $\chi_m \approx 0.022$ at 150 °C; at that temperature we obtained $\chi_m = 0.027$. The higher value of χ_m in our case is due to higher $\bar{y}$;[10,11] $\bar{y}$ for our critical blend is 0.475, and in their results $\bar{y} \approx 0.3$.

Rheological Models Describing LLPS. For Newtonian liquids and their homogeneous mixtures $G' = 0$, but an emulsion of the Newtonian liquids has finite G'.[25−30] This is because, when isotropic emulsion droplets are strained, they deform and store energy, and after the strain is released they return to their isotropic shape, releasing the stored energy, which is measured in terms of G'. In a polymeric system G' is incremented by G'_d when the system phase separates, where G'_d is the storage modulus due to the presence of droplets or due to the interface between the two phases.

The increment in G' due to LLPS is given by Scholz et al.[29] and Gramespacher and Meissner[31] as $G'_d \propto \omega^2\tau_d/(1 + \omega^2\tau_d^2)$, and $\tau_d \propto R$. Here, R is the size and τ_d is the relaxation time of the dispersed phase domains. Therefore, G'_d is prominent at $\omega < 1/\tau_d$, where $G' \propto R$. However, they predict no increment in G'' (G''_d) for $\omega < 1/\tau_d$. The increments in the moduli were also predicted by Ajji and Choplin;[9] however, they also predicted larger effects of LLPS on G' than G''. Onuki[8] predicted that $\Delta\eta^*/\eta^* = A_\eta\phi$, where η^* is the magnitude of the complex viscosity; $\Delta\eta^*$, the increment in η^* due to the LLPS; and ϕ, the volume fraction of the minority phase. The constant A_η varies between 1 and 2. In the terminal region, an increment in η^* implies increases in one or both of G' and G'', because $\eta^* = (G'^2 + G''^2)^{1/2}/\omega$.

In the models of Scholz et al.[29] and Onuki[8] blend components with equal zero-shear viscosities (η_0) are considered. However, if the η_0's are different and follow different time−temperature dependencies, the linear mixing rule to determine the viscosity of phase-separated blends fails. This alone, besides the droplet effects, can contribute to the deviations from homogeneous phase behavior when blends phase separate.[31] Thus, Scholz et al.[29] and Onuki[8] predicted that the increases in G' and G'' (or η^*) are only due to the droplets present in the system. In our HPB/DPB blends, η_0's of the two components are comparable, and also their microstructures are similar. Thus, the rheological effects of LLPS in our blends were mostly due to the presence of droplets and not the failure of the linear mixing rule.[31] Moreover, as the entanglement molecular weights (M_e) of PS (18 000) and PVME (5000) are different, there is a possibility of two different terminal and plateau zones.[3] These effects are practically absent in our blends, as M_e for HPB37 is 2200, and that for HPB58 is 3200.[19] Thus, our HPB/DPB (or HPB/HPB) blends are more suitable than PS/PVME blends for comparison with the models.

Rheology was also used to determined *microphase-separation transition* (MST) temperature (T_{MST}) in block copolymers.[32-38] In block copolymers, MST occurs between *ordered* and *disordered* states. When a block copolymer goes from the disordered to the ordered state, in the terminal region, the exponent of G' vs ω changes from 2 to 0.5, and that of G'' vs ω, from 1 to 0.5. For the ordered state, in a reduced plot (i.e., G' and G'' vs $a_T\omega$), the homogeneous phase behavior is seen for $a_T\omega > a_T\omega_c$, and the deviations are seen for $a_T\omega < a_T\omega_c$. The critical frequency, ω_c, is a characteristic of block copolymer microscopic phase separation.

The rheological LLPS effects depend on the dynamics of droplet relaxation, and the droplet relaxation time is proportional to the droplet radius (R).[29] In block copolymers, the size scale of ordered domains (equivalent to R) remains constant with time and quench depth.[38] However, in blends the droplet size increases with quench depth and time due to coarsening.[21] Therefore, unlike blend LLPS, block copolymer MST exhibits ω_c and a constant exponent (0.5) for G' vs ω and G'' vs ω. Also, MST is a first-order or discontinuous transition, and discontinuities in G' and G'' vs T are present at T_{MST}.[38] This is analogous to the noncritical blend transitions, which were discontinuous in nature, unlike the critical blend transition.

Another interesting application of the rheology of two-phase blends is the determination of interfacial tension (α). In their analysis, Gramespacher and Meissner,[31] Palierne,[39] and Graebling et al.[40] related the increments in G' and G'' to the ratio $\alpha/\bar{R}$, where $\bar{R}$ is an average radius of particles of the dispersed phase. In their analysis, deeply quenched blends of homopolymers were used to effectively calculate α. The blends in our study, due to their shallow quenches, may not have constant size distributions and sizes of the dispersed phase particles, even though the dispersed-phase volume fraction may be constant. However, in a different study,[21] we analyzed a deeply quenched blend of HPB34 ($N_w = 2770$, $N_w/N_n \approx 1.2$) and DPB55 ($N_w = 2530$, $N_w/N_n \approx 1.2$) with $\varphi = 0.75$ to estimate α; the details of the analysis are given elsewhere.[21] The value of α estimated at 50 °C was 0.95 dyn cm^{-1}, which matched with that ($\alpha = 1.56$ dyn cm^{-1}) calculated using the Helfand approach.[41]

Summary

Increases in storage and loss moduli were observed when the HPB/DPB blends phase separated. The effects are reported for a critical (near-critical) and two noncritical blends. The noncritical blends exhibited hysteresis effects unlike the critical blend. As noncritical blends underwent a discontinuous transition and critical blends a continuous transition, an accurate determination of the transition temperature (T_t) was more difficult for the critical blend. The relation between χ_m and T agreed with that obtained by SANS. Our HPB/DPB blends are superior to earlier PS/PVME blends in analyzing the effects of the interface (droplets) in LLPS predicted by Onuki[8] and Scholz et al.[29]

Acknowledgment. I express my sincere gratitude to B. Crist and M. Olvera de la Cruz for their support and helpful discussions and thank J. Rhee for preparing the polymers used in this work. I thank W. W. Graessley, J. Torkelson, and A. Dhinojwala for their critical comments. This work was supported by the David and Lucile Packard Foundation through a fellowship to M. Olvera de la Cruz. Also, acknowledgment is made to the donors of the Petroleum Research Fund, administered by the American Chemical Society, for partial support of the research.

References and Notes

(1) Mazich, K. A.; Carr, S. H. *J. Appl. Phys.* **1983**, *54*, 5511.
(2) Ajji, A.; Choplin, L.; Prud'homme, R. E. *J. Polym. Sci., Part B: Polym. Phys. Ed.* **1988**, *26*, 2279.
(3) Stadler, R.; Freitas, L.; Krieger, V.; Klotz, S. *Polymer* **1988**, *29*, 1643.
(4) Ajji, A.; Choplin, L.; Prud'homme, R. E. *J. Polym. Sci., Part B: Polym. Phys. Ed.* **1991**, *29*, 1573.
(5) Mani, S.; Malone, M. F.; Winter, H. H. *J. Rheol.* **1992**, *36*, 1625.
(6) Han, C. D.; Kim, J. K. *Polymer* **1993**, *34*, 2533.
(7) Winter, H. H. *Makromol. Chem., Macromol. Symp.* **1993**, *69*, 177.
(8) Onuki, A. *Phys. Rev. A* **1987**, *35*, 5149.
(9) Ajji, A.; Choplin, L. *Macromolecules* **1991**, *24*, 5221.
(10) Rhee, J.; Crist, B. *J. Chem. Phys.* **1993**, *98*, 4174.
(11) Graessley, W. W.; Krishnamoorti, R.; Balsara, N. P.; Lohse, D. J.; Fetters, L. J.; Schulz, D. N.; Sissano, J. A. *Macromolecules* **1993**, *26*, 1137.
(12) Ferry, J. D. *Viscoelastic Properties of Polymers*; John Wiley & Sons: New York, 1980.
(13) Larson, R. G. *Rheol. Acta* **1992**, *31*, 497.
(14) Chuang, H.; Han, C. D. *J. Appl. Polym. Sci.* **1984**, *29*, 2205.
(15) Scott, R. L. *J. Polym. Sci.* **1952**, *9*, 423. Krause, S.; Smith, A. L.; Duden, M. *J. Chem. Phys.* **1965**, *43*, 2144. Kambour, R. P.; Bendler, J. T.; Bopp, R. C. *Macromolecules* **1983**, *16*, 753. ten Brinke, G.; Karasz, F. E.; MacKnight, W. J. *Macromolecules* **1983**, *16*, 1827. Paul, D. R.; Barlow, J. W. *Polymer* **1984**, *25*, 487.
(16) Rachapudy, H.; Smith, G. G.; Raju, V. R.; Graessley, W. W. *J. Polym. Sci., Part B: Polym. Phys. Ed.* **1979**, *17*, 1211.
(17) Rhee, J. Ph.D. Thesis, Northwestern University, Evanston, IL, 1992.
(18) Krigas, T. M.; Carella, J. M.; Struglinski, M. J.; Crist, B.; Graessley, W. W.; Schilling, F. C. *J. Polym. Sci., Part B: Polym. Phys. Ed.* **1985**, *23*, 509.
(19) Carella, J. M. Ph.D. Thesis, Northwestern University, Evanston, IL, 1983.
(20) Nesarikar, A.; Olvera de la Cruz, M.; Crist, B. *J. Chem. Phys.* **1993**, *98*, 7385.
(21) Nesarikar, A. R. Ph.D. Thesis, Northwestern University, Evanston, IL, 1994.
(22) Tolédano, J.; Tolédano, P. *The Landau Theory of Phase Transition*; World Scientific: River Edge, NJ, 1987.
(23) Graessley, W. W.; Krishnamoorti, R.; Balsara, N. P.; Butera, R. J.; Fettes, L. J.; Lohse, D. J.; Schulz, D. N.; Sissano, J. A. *Macromolecules* **1994**, *27*, 3896.
(24) Rhee, J.; Crist, B. *Macromolecules* **1991**, *24*, 5663.
(25) Einstein, A. *Ann. Phys. (Leipzig)* **1906**, *19*, 289; **1911**, *34*, 591.
(26) Taylor, G. I. *Proc. R. Soc. London* **1932**, *A138*, 41.
(27) Frölich, H.; Sack, R. *Proc. R. Soc. London* **1946**, *A185*, 415.
(28) Choi, S. J.; Schowalter, W. R. *Phys. Fluids* **1975**, *18*, 420.
(29) Scholz, P.; Froelich, D.; Muller, R. *J. Rheol.* **1989**, *33*, 481.
(30) Krall, A. H.; Sengers, J. V.; Hamano, K. *Phys. Rev. Lett.* **1992**, *69*, 1963.
(31) Gramespacher, H.; Meissner, J. *J. Rheol.* **1992**, *36*, 1127. Meissner, J. *Makromol. Chem., Macromol. Symp.* **1993**, *68*, 133.
(32) Chung, C. I.; Gale, J. C. *J. Polym. Sci., Part B: Polym. Phys. Ed.* **1976**, *14*, 1149.
(33) Gouinlock, E. V.; Porter, R. S. *Polym. Eng. Sci.* **1977**, *17*, 535.
(34) Chung, C. I.; Lin, M. I. *J. Polym. Sci., Part B: Polym. Phys. Ed.* **1978**, *16*, 545.
(35) Bates, F. S. *Macromolecules* **1984**, *17*, 2607.
(36) Han, C. D.; Kim, J.; Kim, J. K. *Macromolecules* **1989**, *22*, 383.
(37) Rosedale, J. H.; Bates, F. S. *Macromolecules* **1990**, *23*, 2329.
(38) Bates, F. S. *Science* **1991**, *251*, 898.
(39) Palierne, J. F. *Rheol. Acta* **1990**, *29*, 204.
(40) Graebling, D.; Muller, R.; Palierne, J. F. *Macromolecules* **1993**, *26*, 320.
(41) Helfand, E.; Sapse, A. M. *J. Chem. Phys.* **1975**, *62*, 1327.

MA950339J